

Supplementary Information

*CO₂ Binding on Pt(111) Under an Applied Electric Field

In DFT calculations, CO₂ can bind to Pt(111) in a chemisorbed state in a bridged configuration through the carbon and oxygen atoms. Figure S1 shows the binding energy of CO₂ on Pt(111) at various applied external fields. Binding energies are calculated by subtracting the electronic energy of a bare slab under a field and a reference gas phase energy from the electronic energy of the adsorbate-slab system under the same applied field.

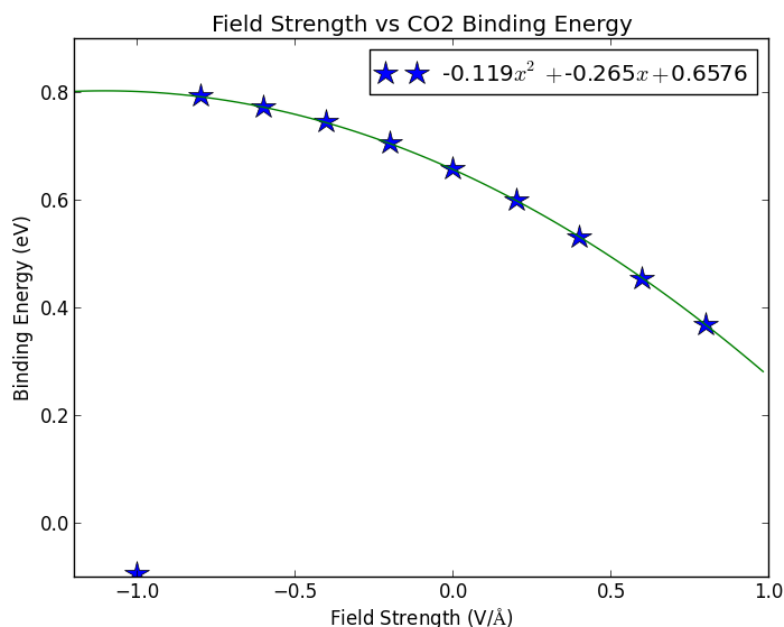


Figure S1. CO₂ binding energy versus applied electric field strength over a range of potentials relevant to electrochemistry. Reference gas phase energy used is the electronic energy of CO₂.

At field strengths negative of -0.8 V/Å , adsorbed CO₂ desorbs spontaneously in a geometry optimization. At field strengths positive of 0.8 V/Å , the electrostatic potential in the vacuum is so strong that electron density is pulled out of the slab-adsorbate system into the vacuum. At electrochemically reducing potentials, excess electron density would be pulled from the bulk into the surface, which can loosely be represented by an applied electric field strength in the positive direction. We note that the binding strength of CO₂ increases as the applied electric field becomes stronger. Therefore, we would expect the binding strength to also increase under more cathodic potentials in CO₂ reducing conditions.

Additionally, we note that although applying a positive external electric field increases the electron density in the surface atoms and adsorbate, the electronic density seen in the charged adsorbate-slab-water layer system cannot be replicated at any field. This is due to the presence of an extra electron in the slab-adsorbate layer when the capacitor is charged, allowing the formation of somewhat of a

negatively charged and very stable adsorbed species, e.g. $^*\text{CO}_2^{(-)}$. The (highly endothermic) binding energies shown in Figure S1 are not intended to be taken at face value, as the bound state of CO_2 even under a field is not an accurate interpretation of the bound state in an electrochemical system, which would be a much more stable $^*\text{CO}_2^{(-)}$. The important insight given by the applied field study is the trend of stronger binding at more positive applied fields or negative potentials.

Thermodynamics of Other Possible Pathways on Pt(111)

In Figure 1, we show the minimum-energy pathway from the 8-electron reduction of CO_2 to methane. However, as extensive previous work has shown¹, there are a vast array of possible CO_2 reduction intermediates. We have neglected these other possible intermediates due to their instability on the Pt(111) surface. Figure S2 below shows a more complete picture of possible CO_2 reduction intermediates.

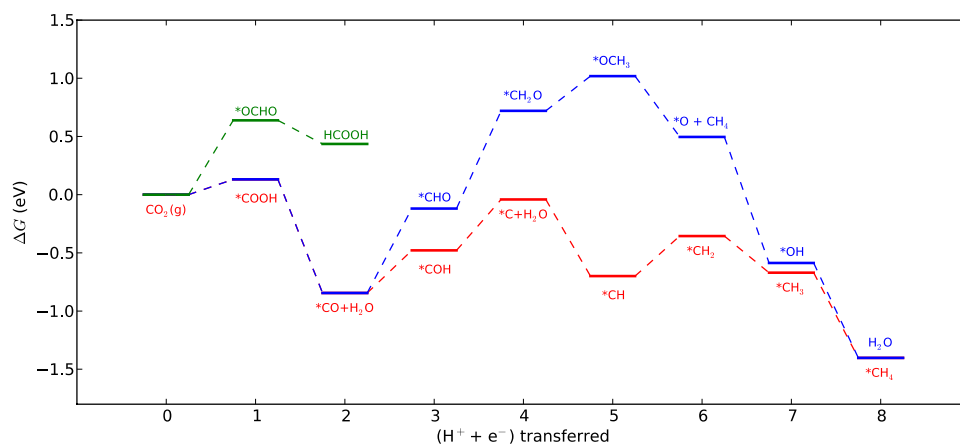


Figure S2. Free energy diagrams for the electrochemical reduction of CO_2 to CH_4 and HCOOH on Pt(111) using the Computational Hydrogen Electrode at 0V vs. RHE. These results show that the pathways relying on the formation of $^*\text{OCHO}$ and $^*\text{CHO}$ are thermodynamically disfavored compared to the pathway to methane formation through $^*\text{COH}$ on the Pt(111) surface.

Work Functions Changes and Charge Densities of $^*\text{COH}$ to $^*\text{C}$

Although the $^*\text{CO}$ to $^*\text{COH}$ elementary step is the first possible potential-limiting step to methane formation on Pt(111), according to Figure 1, the next step, $^*\text{COH}$ to $^*\text{C}$, is just as uphill and also likely to be potential limiting. It is important to understand why the barrier appears to be higher for this step as well as origin of the large work function change (2.17 eV) that occurs.

If we examine the work function at each NEB image in Figure 8, we find that 80% of the work function change from initial state to final state has already occurred at the transition state, “TS”. The water layer relaxation causes a change in energy, but not much of a change in work function. We can examine this system in even more detail by doing the same charge density analysis used for Figure 9 on the $^*\text{CO}$ to $^*\text{COH}$ elementary step. the electron density difference shown, $\Delta \rho$, is:

$$Dr = r_{\text{system}} - r_{\text{slab+C}} - r_{\text{OH}} - r_{\text{water layer}} - r_{\text{extra hydrogen}}$$

where ρ_{OH} refers to the charge density of the OH in *COH. Figure S3 shows the result of this analysis.

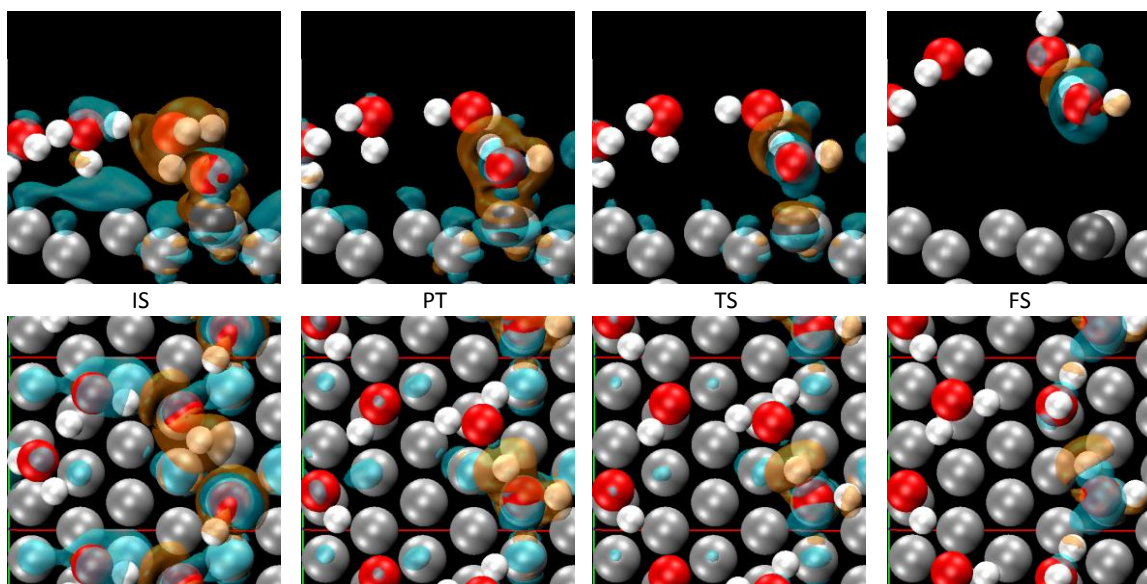


Figure S3. Side (upper) and top (lower) views of isosurface electron density diagrams for the proton-electron transfer to *COH to make *C and H₂O on Pt(111). Orange regions represent missing electron density iso-values of $-0.004 e^- \text{ Bohr}^{-3}$ relative to the reference state. Cyan regions represent excess electron density iso-values of $+0.0025 e^- \text{ Bohr}^{-3}$ relative to the reference state. Total electron density relative to the reference state sums to 0. Each image has the same atomic configuration as the corresponding images in Figure 8.

From these charge density diagrams we notice a key difference between Figure S3 and Figure 9 that can help explain both the increase in barrier of proton transfer and the increased change in work function. In the initial state, the charged system of *COH does not have the extra hydrogen atom's electron localized on the adsorbate as was the case in charged *CO. That extra electron is instead delocalized on the surface of the platinum atoms, and during the proton transfer, there is a simultaneous electron transfer from the surface to form the new O-H bond of the H₂O product. This large concerted movement of electrons density is responsible for the large change in work function and the higher barrier to protonation of the oxygen, whereas in the previous step of *CO to *COH shown by Figure 9, electron density barely shifted in what could be considered almost like a surface acid-base reaction.

Density of States of *CO₂(⁻)

In Figure S4 below, we plot the atom projected density of states for the adsorbed *CO₂ in the initial (charged) state of Figure 3. The projected density of states is plotted using a Gaussian smearing with a width of 0.2 eV. The adsorbate states are broadened to a width of the order of 1 eV, implying that the electron transfer is barrierless and fast relative to the proton transfer.²

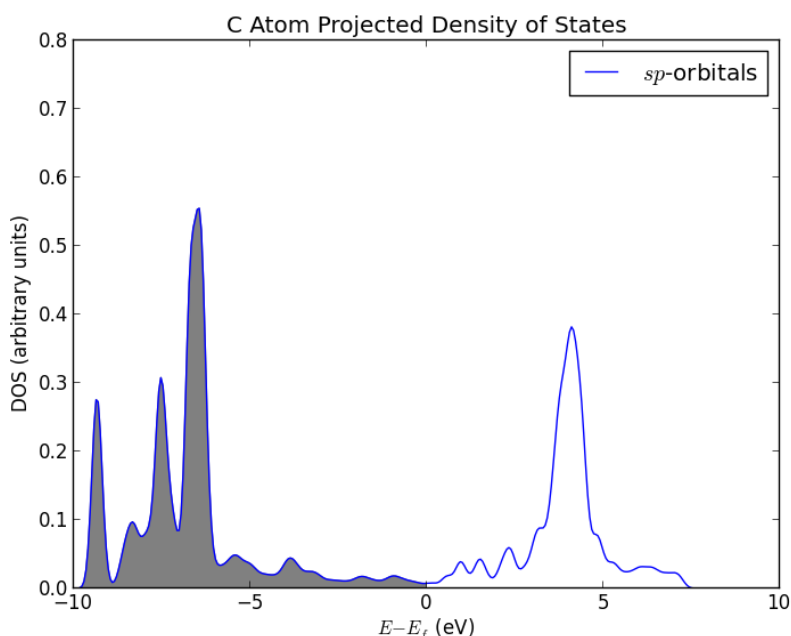


Figure S4. Density of states projected onto to sp states of the carbon atom of $*CO_2$ in a charged water layer on $Pt(111)$.

Free Energy Corrections

All barriers and energies presented in the main work are electronic energies. In this section, we show that changing the analysis to use free energies rather than electronic energies does not significantly change the conclusions made. All Free energies were obtained by using the calculated vibrational frequencies for the surface atoms (Pt and adsorbates) and the transferred hydrogen in the harmonic limit for a temperature of 298.15K. Table S5 below shows the results of the analysis.

Reaction Step Number	Elementary Reaction	ΔE^\ddagger (eV)	ΔG^\ddagger (eV)
1	$*CO_2 + H^+ + e^- \Rightarrow *COOH$	0.08	0.09
2	$*COOH + H^+ + e^- \Rightarrow *CO + H_2O$	0.48	0.39
3	$*CO + H^+ + e^- \Rightarrow *COH$	0.09	0.06
4	$*COH + H^+ + e^- \Rightarrow *C + H_2O$	0.53	0.65

Table S5. Electronic and Free energies of transition states relative to initial states of the first four elementary steps of CO_2 reduction on $Pt(111)$.

We find that the additional correction made to the electronic energy for the transition state to obtain a free energy is consistently on the order of 0.1 eV and does not significantly change the conclusions made about the likelihood of any of these elementary steps being rate-limiting in electrochemical conditions.

References

1. A. a. Peterson, F. Abild-Pedersen, F. Studt, J. Rossmeisl, and J. K. Nørskov, *Energy & Environmental Science*, 2010, **3**, 1311.
2. W. Schmickler, *Journal of Electroanalytical Chemistry and Interfacial Electrochemistry*, 1986, **204**, 31–43.